

Unexpected sustained soil carbon flux in response to simultaneous warming and nitrogen enrichment compared with single factors alone

Received: 26 July 2023

Accepted: 23 August 2024

Published online: 24 September 2024

 Check for updates

Melissa A. Knorr^{1,2}✉, A. R. Contosta^{1,2,3}, E. W. Morrison^{1,2}, T. J. Muratore^{1,2}, M. A. Anthony⁴, I. Stoica⁵, K. M. Geyer⁶, M. J. Simpson^{1,2} & S. D. Frey^{1,2}✉

Recent observations document that long-term soil warming in a temperate deciduous forest leads to significant soil carbon loss, whereas chronic soil nitrogen enrichment leads to significant soil carbon gain. Most global change experiments like these are single factor, investigating the impacts of one stressor in isolation of others. Because warming and ecosystem nitrogen enrichment are happening concurrently in many parts of the world, we designed a field experiment to test how these two factors, alone and in combination, impact soil carbon cycling. Here, we show that long-term continuous soil warming or nitrogen enrichment when applied alone followed the predicted response, with warming resulting in significant soil carbon loss and nitrogen fertilization tending towards soil carbon gain. The combination treatment showed an unanticipated response, whereby soil respiratory carbon loss was significantly higher than either single factor alone, but without a concomitant decline in soil carbon storage. Observations suggest that when soils are exposed to both factors simultaneously, plant carbon inputs to the soil are enhanced, counterbalancing soil carbon loss and helping maintain soil carbon stocks near control levels. This has implications for both atmospheric CO₂ emissions and soil fertility and shows that coupling two important global change drivers results in a distinctive response that was not predicted by the behaviour of the single factors in isolation.

Manipulative global change experiments are used to understand how anthropogenic environmental change is impacting Earth's ecosystems. They provide input data for ecosystem and Earth-system models used to predict how ecosystems may respond to future changes in the environment. These experiments generate hypotheses upon which to build future research, and they inform society, including policymakers, about the consequences of global change. Most global change experiments are short-term (<5 years) and single factor (70–80%

of all published studies)^{1,2}, whereby one treatment (for example, warming, elevated CO₂, drought, nitrogen enrichment) is compared with the control condition. However, we reside in a multifactor world in which many environmental changes are occurring simultaneously and may interact in ways that cannot be predicted from single-factor studies². Multifactor experiments are thus needed to provide insight into how ecosystems may respond to current and future interacting global change drivers.

A full list of affiliations appears at the end of the paper. ✉ e-mail: mel.knorr@unh.edu; serita.frey@unh.edu

We focus in this article on soils, which play a critical role in the climate system by sequestering carbon as soil organic matter (SOM), the largest repository of carbon in the terrestrial biosphere³. Soils are also critical for ecosystem productivity because they are an important reservoir of plant-available nutrients. Forest soils store nearly half of all soil carbon globally⁴, thereby offsetting a substantial portion of greenhouse gas forcing of the climate system. Current soil carbon stocks are under threat from anthropogenic stressors, which act to alter the balance between plant carbon inputs to soil and respiratory carbon outputs to the atmosphere through SOM decomposition. Climate warming and atmospheric nitrogen deposition, which are currently +1.1 °C (ref. 5) and up to 10 times⁶ above pre-industrial levels respectively, are widely recognized as two of the most impactful global change pressures⁷. These two factors have also been established as key drivers of temperate forest soil carbon storage. Long-term soil temperature increases typically lead to significant soil carbon loss through enhanced microbial-mediated SOM decomposition^{8,9}, with potential positive feedback to the climate system. By contrast, nitrogen enrichment of temperate forest soils results in significant soil carbon gain^{10–14} via suppression of SOM decomposition^{10,15}. Divergent responses to warming versus nitrogen enrichment make it difficult to predict the net impact on soil carbon stocks in a multifactor world in which these two global change factors are occurring simultaneously, and few long-term studies have examined how these two factors interact to influence soil carbon dynamics. Thus, the long-term sensitivity of SOM decay to changing temperatures and soil nitrogen availability are highly uncertain, and without long-term, multifactor field-based experiments the directionality, magnitude and mechanisms of carbon–nitrogen–climate feedbacks remain unidentified.

Here, we conducted a long-term field experiment within a temperate forest located at the Harvard Forest Long-term Ecological Research (LTER) site in Massachusetts, United States, where soil was continuously warmed (+5 °C), fertilized (+5 g N m⁻² yr⁻¹) or warmed and fertilized at the same levels as the single-factor treatments (Methods). First, we analysed the soil respiratory carbon loss (CO₂ flux) over 16 years of long-term soil warming, nitrogen enrichment or their combination. We then assessed cumulative respiratory carbon loss and compared this with the amount of carbon stored as organic matter in the soil profile. Finally, we documented microbial and root responses to the experimental treatments to provide mechanistic understanding for observed changes in soil carbon cycling. Previous work from single-factor experiments adjacent to our site showed that 26 years of soil warming (+5 °C) resulted in a 17% loss of soil carbon from the top 60 cm of the soil profile⁸. By contrast, two decades of soil nitrogen enrichment at a nearby experiment in the same forest (same vegetation, soil type and climate) led to significant soil carbon gain caused by suppression of microbial decomposition of SOM¹⁰. We thus anticipated that with simultaneous soil warming and nitrogen enrichment, increased soil nitrogen availability would offset heating-induced soil respiratory carbon loss. Contrary to expectations, we found that soil CO₂ emissions in the combination treatment (heated × N) were significantly higher than either single factor alone, but soil carbon storage was not significantly different from the control condition, potentially because of unique shifts in microbial community and root dynamics.

Results and discussion

Soil respiratory response

To assess the soil respiratory response to the experimental treatments, we quantified annual soil carbon loss associated with carbon dioxide flux (that is, the carbon component of soil respiration; CO₂-C) emissions over 16 years (Fig. 1a) by directly measuring autotrophic (root, mycorrhizal fungi) plus heterotrophic (microbial) respiration over the growing season (May to October) (Extended Data Fig. 1) and calculating annual emissions using continuously collected soil temperature data (Methods and Extended Data Figs. 2 and 3). Nitrogen fertilization in

the absence of warming (nitrogen-only treatment) resulted in an initial enhancement of soil respiration that dampened within five years of experiment initiation. After this initial period, the respiratory response was not significantly different from control plots for the last 12 years of the study (Fig. 1a). In addition, soil respiration trended lower than control plots after 15 years of fertilization, consistent with previous research in a separate, single-factor experiment at the same site documenting a suppression of soil respiration after two decades of nitrogen enrichment¹⁰. This initial increase and eventual decrease in soil respiration from the nitrogen-only treatment plots resulted in a cumulative respired carbon loss that was only 6% higher than the control (Fig. 1b). Warming, alone or in combination with nitrogen addition, significantly elevated soil respiration relative to the control across almost all years of the study. The magnitude of this elevated CO₂ flux was greatest when warming and nitrogen addition were combined (heated × N), resulting in 26% more cumulatively respired CO₂-C compared with the control condition, whereas the single-factor treatment (heated only) respired 17% more carbon relative to the controls over the duration of the experiment (Fig. 1b). Treatment differences for instantaneous soil respiration rates were consistent with these observations, particularly with respect to enhanced CO₂-C fluxes in response to warming, both with and without added N (Extended Data Figs. 1 and 4 and Extended Data Table 1). Similar to a single-factor warming study at the same site⁸, we observed a cyclic pattern in soil respiration across all plots (including controls) that reflects patterns of ambient climate, particularly annual average soil temperature (Extended Data Fig. 2). Thermal acclimation, a phenomenon observed previously in response to soil warming at our site^{8,16}, was evident for both warming treatments (heated, heated × N), such that at a given temperature there was less respiration from heated compared with control plots (Fig. 1c). However, this acclimation was insufficient to compensate for the 5 °C increase in soil temperature, resulting in CO₂ emissions being consistently greater from the heated treatment than the control treatment.

Soil organic matter storage

Enhanced soil respiration with long-term warming was accompanied by a 23% decline in total soil organic matter-carbon (SOM-C) stored within the soil profile (Fig. 2a), consistent with previous work in an adjacent single-factor warming experiment at our site⁸, experiments at other sites⁹ and meta-analyses of 161 (ref. 1) and 85 (ref. 17) field warming experiments located across North America, Europe and Asia. This loss was primarily driven by a significant loss (46%) of carbon in the organic horizon (Extended Data Table 2). There was a trend towards increased SOM-C storage under soil nitrogen enrichment, although this was only significant in the mineral soil at depth (10–20 cm; Extended Data Table 2). This result is in line with previous work at a nearby single-factor nitrogen fertilization study in which there was significant SOM-C accumulation following two decades of chronic soil nitrogen enrichment at the same level of addition (5 g N m⁻² yr⁻¹)¹⁰. Contrary to expectation, high soil respiration within the combination treatment (heated × N; Fig. 1) did not translate into anticipated SOM-C loss (Fig. 2a). Soil carbon storage was not significantly different relative to the control when soil was simultaneously heated and fertilized, and indeed, SOM-C was significantly higher (+36%) in the mineral soil at depth (10–20 cm), as seen for the nitrogen-only treatment (Extended Data Table 2). These results suggest that autotrophic (root, mycorrhizal fungal) respiration and/or plant carbon inputs are enhanced with the combination (heated × N) treatment such that soil respiration rates are maintained at a high level without a concomitant loss of SOM-C. This led us to explore potential mechanisms underlying this unexpected finding.

Microbial and root mechanisms underlying soil C dynamics

We first measured SOM chemistry using solid-state ¹³C nuclear magnetic resonance (¹³C-NMR) spectroscopy to assess the degree of degradation (alkyl to O-alkyl C ratio; Extended Data Table 3) caused

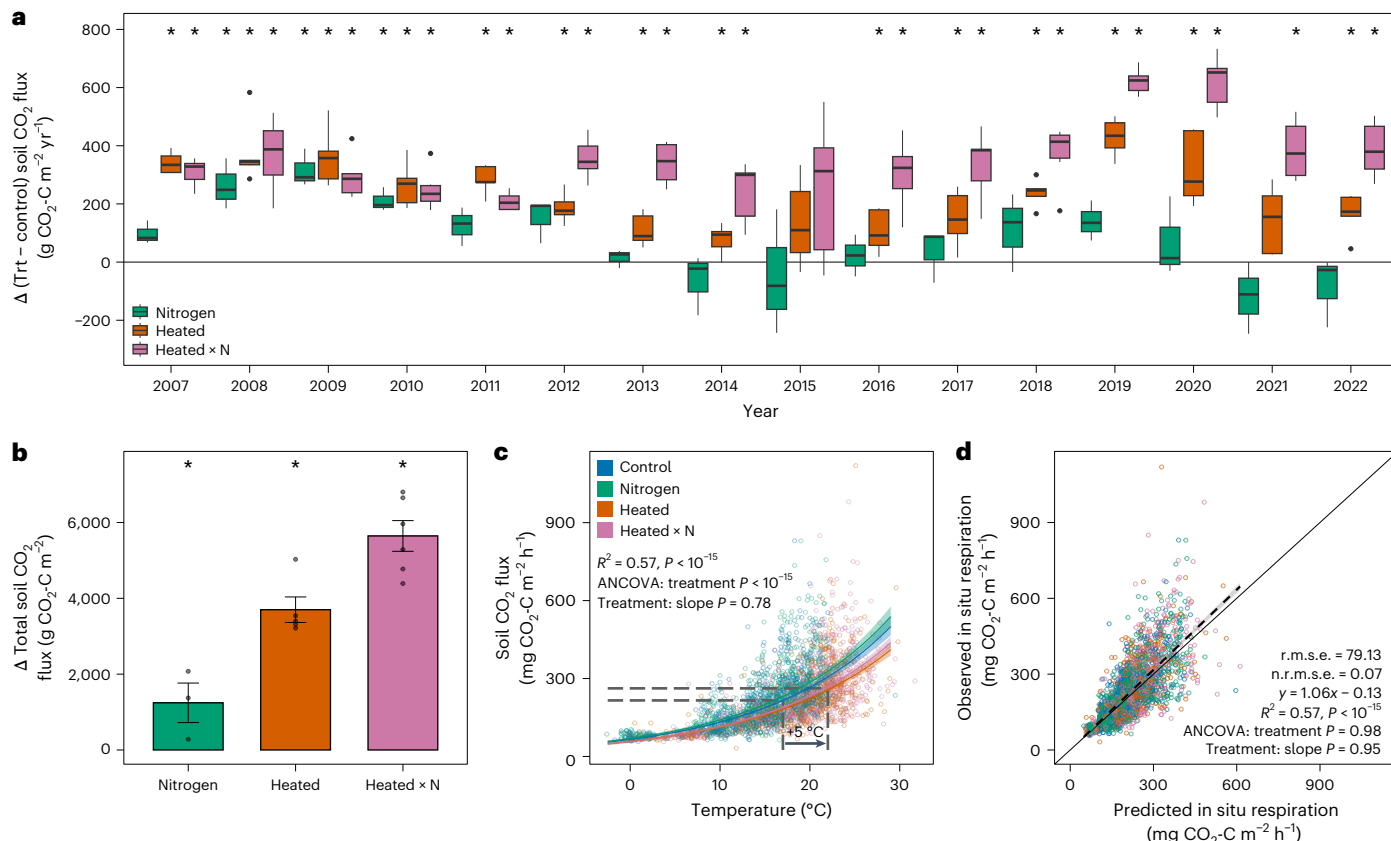


Fig. 1 | Soil respiratory response to long-term warming, N enrichment or their combination. **a**, Empirically modelled annual soil CO_2 flux from treatment (Trt) relative to control plots over 16 years of experimental treatment. Asterisks indicate significant pairwise differences from control plots according to two-sided t -tests. The boxplot centre line indicates the median, the box indicates the 25th and 75th percentiles (interquartile range (IQR)) and the whiskers indicate the smallest and largest values, respectively, within $1.5 \times \text{IQR}$. Outliers beyond $1.5 \times \text{IQR}$ are indicated by points. **b**, Empirically modelled cumulative loss of soil $\text{CO}_2\text{-C}$ (mean \pm s.e.) over the full 16-year study relative to control plots, which for reference, respired $21.4 \text{ kg CO}_2\text{-C m}^{-2}$ over this duration. All treatments are significantly different from the control according to two-way ANOVA and Tukey's HSD correction (nitrogen $P = 0.007$, heated $P < 10^{-7}$, heated \times N $P < 10^{-7}$). In **a** and **b** the empirical model was parameterized using instantaneous respiration and temperature measurements from six independent replicate plots in all treatments except the heated treatment ($n = 5$). For the nitrogen-only treatment, $n = 3$ because hourly long-term temperature measurements were performed in three of the six replicate plots for prediction of annual flux and subsequent statistics. **c**, Instantaneous respiration as a function of soil temperature (points) with trendlines modelled as an exponential function of soil temperature:

$R_s = Ae^{kT_s}$, where A represents respiration at 0°C and k represents the temperature sensitivity of soil respiration. Analysis of covariance (ANCOVA) results confirm lower average respiration at a given temperature in the heated treatments (nitrogen intercept $P = 0.28$, heated $P = 0.022$, heated \times N $P = 0.016$), but no difference in the slope of the temperature–respiration relationship among treatments (the interaction term is not significant, $P = 0.78$). Dashed lines represent the predicted soil respiration rate when unheated plots are 17°C and heated plots are 22°C , the respective average summer temperatures. Shading around the trendlines represents 95% confidence intervals. **d**, Comparison of observed and predicted values with measures of model accuracy (embedded text). The dashed line represents the linear trend. Predictions were generated using the same temperature measurements that were used to parameterize the empirical temperature–respiration model and the resulting model coefficients are shown. ANCOVA represents analysis of variance of the effect of treatment on the relationship between predicted and observed values indicating no effect of treatment on either slope ($P = 0.95$) or intercept ($P = 0.98$). Accuracy measures (root mean squared error (r.m.s.e.), normalized root mean squared error (n.r.m.s.e./range [y]), R^2) indicate a good fit of the model to the data.

by microbial decomposition of SOM¹⁸. Long-term nitrogen fertilization (nitrogen-only treatment) suppressed SOM degradation (Fig. 2b), consistent with previous work showing that chronic soil nitrogen enrichment suppresses SOM decomposition in temperate deciduous forests^{10,19,20}. SOM chemistry revealed that O-alkyl carbon, which is associated with cellulose and other readily decomposable microbial substrates, was higher in both the organic horizon and mineral soil for the nitrogen-amended plots (Extended Data Table 3), suggesting the accumulation of otherwise easily decomposable forms of SOM for this experimental treatment. A comparison of SOM composition via NMR also indicated that nitrogen addition reduced overall SOM resistance to decomposition compared with the control plots (Extended Data Table 3). In addition, several other plant-derived compounds were enriched under nitrogen addition, demonstrating the accumulation of intact plant biopolymers that are otherwise easily decomposed^{18,21,22}.

These changes in SOM chemistry align with our finding of suppressed soil CO_2 fluxes (Fig. 1) and elevated SOM-C storage (Fig. 2a), but also demonstrate that chronic soil nitrogen enrichment alone may reduce the potential for long-term SOM persistence because less-stable forms of SOM accumulate that may be less resistant to future environmental change.

With long-term soil warming (heated-only treatment), SOM decomposition, as determined by ^{13}C -NMR, was elevated relative to control plots in the organic horizon (Fig. 2b), consistent with significant loss of carbon from this horizon (Fig. 2a), along with elevated soil CO_2 emissions (Fig. 1). Thus, soil warming and nitrogen enrichment, when applied as single-factor treatments, alter the biogeochemical trajectory of SOM in opposite directions (accelerated degradation versus preservation, respectively) consistent with patterns of soil respiration and SOM loss (warming) or storage (nitrogen addition). When these global

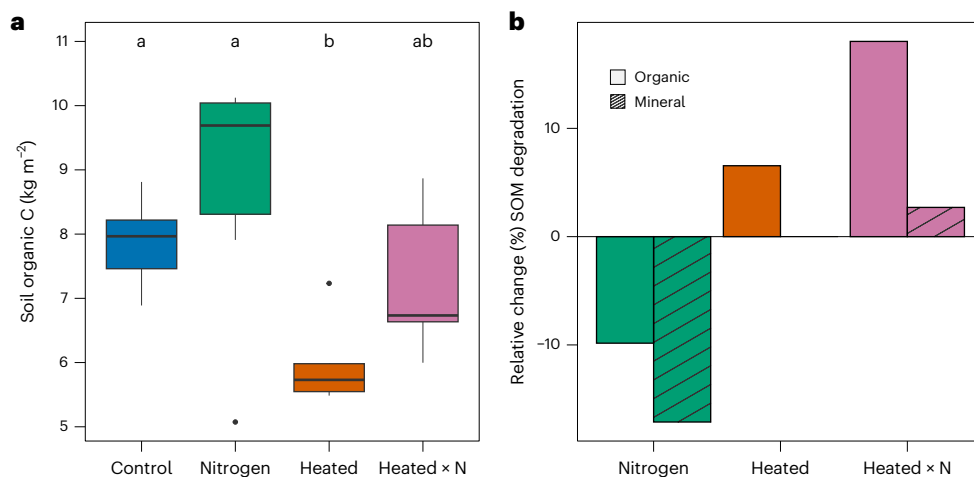


Fig. 2 | SOM responses to long-term warming, N enrichment or their combination. **a**, Total SOM-C stocks ($n = 6$ for all treatments except the heated treatment where $n = 5$). The boxplot centre line indicates the median, the box indicates the 25th and 75th percentiles (IQR) and the whiskers indicate the smallest and largest values respectively, within $1.5 \times \text{IQR}$. Outliers beyond $1.5 \times \text{IQR}$ are indicated by points. Significant differences as determined by two-way ANOVA and Tukey's HSD are indicated by different letters, a, b and ab, such that control

and nitrogen plots are different from heated but not heated \times N plots (control vs. heated: $P < 0.001$; nitrogen vs. heated: $P < 0.001$). **b**, Relative (to control plots) per cent difference in SOM degradation as measured by the solid-state ^{13}C -NMR alkyl to O-alkyl C ratio. **a** shows results across the soil profile (organic horizon and 0–20 cm mineral soil), whereas **b** shows results separately for the organic horizon and mineral soil.

Table 1 | Mass-specific microbial respiration and carbon-use efficiency

Response variable	Experimental treatment			
	Control	Nitrogen	Heated	Heated \times N
Specific respiration ($\mu\text{g C g}^{-1} \text{MBC}$)	0.03 (0.01) ^a	0.03 (0.01) ^{ab}	0.07 (0.01) ^b	0.05 (0.01) ^{ab}
Carbon-use efficiency	0.18 (0.04)	0.15 (0.05)	0.10 (0.02)	0.10 (0.02)

Mass-specific respiration and carbon-use efficiency were determined by ^{18}O incorporation into microbial DNA^{55,56}. Mass-specific respiration, two-way ANOVA, main effect of heating $P = 0.004$. MBC refers to microbial biomass carbon. Significance is denoted by the letters a, b and ab, where only control and heated plots are significantly different.

change drivers are combined (heated \times N), an unexpected dynamic occurs, whereby SOM degradation is enhanced in both the organic horizon and mineral soil above that seen for heating alone (Fig. 2b). Previous work at our site, pairing NMR data with corroborating, sensitive molecular assays, documented that the magnitude of SOM degradation in the combination treatment intensifies over time, but also exhibits patterns that are distinct from the individual treatments^{18,21,22}. Thus, there is a new mechanism that maintains SOM-C levels in the heated \times N treatment while still eliciting greater SOM degradation and a higher soil CO_2 efflux than was anticipated based on behaviour observed in the single-factor treatments.

Characterization of the soil microbial community suggests changes in microbial physiology and community composition that help explain the NMR signature of greater SOM degradation in the combination (heated \times N) treatment relative to the others (Fig. 2b). Physiological assays documented a more active, but less efficient microbial community with warming (with or without added nitrogen), where specific microbial respiration (soil CO_2 flux per unit biomass) was significantly higher ($P = 0.004$) and carbon-use efficiency lower ($P = 0.109$) in heated relative to unheated plots (Table 1), in line with the NMR results showing greater SOM degradation in response to long-term warming (Fig. 2b). The soil microbial community at Harvard Forest is dominated by fungi, which make up >90% of the total and ~65% of the active microbial biomass²³. Thus, fungi are the primary decomposers at the site and drive SOM degradation. Although fungal biomass was not significantly different across experimental treatments²⁴, the composition of the saprotrophic (decomposer) component of the community shifted in the combination (heated \times N) treatment towards one that is distinct from

both the control and single-factor treatments (Extended Data Fig. 5). There is a significantly higher relative abundance of fungal hydrolytic enzyme encoding genes in the heated \times N plots compared with the other treatments²⁴, potentially linked to greater SOM decomposition. The response observed for fungal saprotrophs was not observed for other components of the fungal community (ectomycorrhizal fungi, arbuscular mycorrhizal fungi, plant pathogens). Because saprotrophic fungi are the primary decomposers of SOM-C at this site, their response plus enhanced potential for fungal hydrolytic enzyme biosynthesis suggests that changes in the microbial community and substrate utilization patterns are fundamentally and uniquely altering SOM decomposition pathways under simultaneous warming and nitrogen addition. Soil microbial communities have been observed previously to reorganize with warming^{25–28} or nitrogen fertilization^{29–32} but have rarely been examined under both stressors simultaneously.

Finally, we examined the response of plant roots (Methods), which contribute to soil carbon loss (CO_2 emissions) directly through root and mycorrhizal fungal respiration and indirectly by stimulating heterotrophic microbial activity in the rhizosphere. We find that long-term warming, with or without added nitrogen, significantly reduced the amount of fine root biomass across the soil profile (Fig. 3a). In addition, mass-specific root respiration rates were significantly decreased under warming but returned to control levels when N was applied simultaneously (Extended Data Fig. 6). Given the reduction in root biomass and the change in physiology at the root level, we scaled mass-specific root respiration rates to the ecosystem level by accounting for the biomass of roots in each plot³³ (Methods). Ecosystem root respiration was significantly reduced under the single-factor treatments (heated

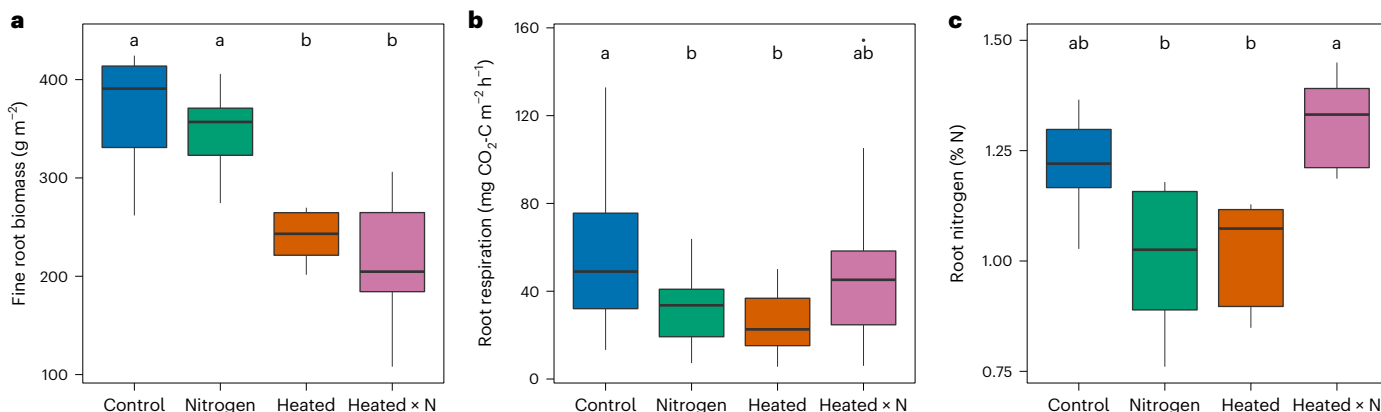


Fig. 3 | Root responses to long-term warming, N enrichment or their combination. **a**, Fine root biomass (<2 mm) for the combined organic and mineral soil horizons (0–20 cm). **b**, Ecosystem root respiration. **c**, Fine root N content. The boxplot centre line indicates the median, the box indicates the 25th and 75th percentiles (IQR) and the whiskers indicate the smallest and largest values, respectively, within 1.5× IQR. $n = 6$ in all treatments except the

heated treatment where $n = 5$. Significant differences as determined by two-way ANOVA and Tukey's HSD are indicated by different letters (control vs. heated $P = 0.0077$, control vs. heated \times N $P = 0.0009$, nitrogen vs. heated $P = 0.0269$, nitrogen vs. heated \times N $P = 0.0035$ (**a**); control vs. nitrogen $P = 0.035$, control vs. heated $P < 0.001$ (**b**); nitrogen vs. heated \times N $P = 0.0049$, heated vs. heated \times N $P = 0.0087$ (**c**)).

or nitrogen-only), but simultaneous treatment with these two factors (heated \times N) ameliorated this effect, with root respiration in the combination treatment not significantly different from the control (Fig. 3b). This pattern of root respiration corresponds to that of root nitrogen concentrations which in the combination treatment (heated \times N) were not significantly different from the control, but were significantly higher than in either single-factor treatment (Fig. 3c). Root nitrogen content has been shown to positively correlate with root respiration^{33–37} and turnover rates³⁸. Furthermore, changes in root tissue N content may be caused by shifts in functional class (absorptive versus transport), predominant root species identity or a combination of these factors. Although warming reduced root biomass (Fig. 3a) in both the heated and heated \times N treatments, respiration rates were less constrained by the interaction of warming with N addition^{33,39}. Taken together, the elevated ecosystem root respiration rates in the heated \times N plots can help account for the overall heightened soil respiration rates. Nonetheless, the mechanisms sustaining soil organic carbon stocks at control levels remain poorly understood. Although we observed reduced fine root biomass in the combination treatment, the probable higher root turnover rates, as indicated by increased root N concentration, could stimulate autotrophic respiration by a proliferation of younger roots, along with the production of root exudates^{40,41}. The latter would in turn stimulate heterotrophic respiration, helping explain enhanced in situ respiration in the combination treatment (heating \times N) over the long term.

Increased plant carbon inputs also can contribute to SOM formation, whereby root-derived carbon, including that associated with mycorrhizal fungal hyphae, is a dominant pathway through which carbon enters the SOM pool, contributing as much or more to long-term soil carbon storage as aboveground plant components^{42–45}. Evidence in our study for elevated inputs of root carbon to the total SOM pool is supported by soil chemistry data showing significantly higher amounts of suberin-derived compounds with warming, both with and without added nitrogen²², potentially signalling enhanced root production and turnover rates in warmed soils. Taken together, we hypothesize that simultaneous long-term soil warming and nitrogen enrichment enhance plant root turnover and/or exudation in such a way that plant carbon inputs counterbalance soil carbon loss (that is, soil CO_2 emissions) accelerated by a saprotrophic fungal community with greater hydrolytic enzyme biosynthesis investments²⁴ that decompose fresh plant inputs instead of stable SOM, helping maintain the total SOM

pool near control levels. This hypothesis is currently being evaluated in a follow-up study.

In conclusion, our work highlights the importance of long-term, multifactor experiments for accurately predicting soil carbon dynamics in an era in which ecosystems are experiencing multiple global change factors concurrently (Extended Data Table 4). In systems in which nitrogen availability is enhanced through fertilization or atmospheric nitrogen deposition, SOM loss in response to warming may be less than previous estimates obtained from single-factor warming studies, having implications for soil fertility and ecosystem productivity. In addition, if elevated rates of soil respiration under warmed and nitrogen-enriched conditions are dominated by plant-derived soil carbon inputs rather than the mineralization of SOM, the potential feedback to the climate system may be less than previously predicted, with CO_2 fluxes to the atmosphere being offset by enhanced gross primary productivity.

Methods

Site characteristics

The Soil Warming \times Nitrogen Addition Study, initiated in 2006, is located at the LTER site in Petersham, MA, United States (42.54, -72.18) in an even-aged, mixed deciduous forest dominated by American beech (*Fagus grandifolia*), white birch (*Betula papyrifera*), red maple (*Acer rubrum* L.), striped maple (*A. pensylvanicum* L.), red oak (*Quercus rubra*) and black oak (*Q. velutina* Lam.)⁴⁶. Mean annual temperature is 7 °C but can vary from a high of 32 °C in summer to a low of -25 °C in winter. Mean annual precipitation is evenly distributed across the year, averaging 1,100 mm (Extended Data Fig. 2)⁴⁷. Soils are fine loamy, mixed, mesic Typic Dystrudepts of the Gloucester series with pH of 3.8 and 4.3 in the organic horizon and mineral soil (0–10 cm), respectively. Soils are shallow, with rocky glacial deposits starting within 20–30 cm of the soil surface. The experimental design consists of twenty-four 3 m² plots with six replicates each of four treatments: control, which receives no manipulation; heated, in which soil (surface to >30 cm depth) is warmed continuously to 5 °C above ambient soil temperatures by resistance cables buried at 10 cm depth and spaced 20 cm apart; nitrogen, in which treatment plots receive an aqueous addition of NH_4NO_3 at a rate of 50 kg N ha⁻¹ yr⁻¹ applied in six monthly doses of 500 ml (non-fertilized plots receive 500 ml of water only) throughout the growing season (May to October); and heated \times N, which receives both warming (+5 °C) and N addition (50 kg N ha⁻¹ yr⁻¹). There are only

five replicates sampled for heated-only plots currently, because wiring damage occurred in 2009 to one replicate plot, and this plot is no longer maintained or sampled.

In situ soil respiration

Soil (root and microbial) respiration was measured monthly throughout the growing season (May to October) in all years using a static chamber (2006–2011)⁴⁸ or LI-COR LI-8100-a portable CO₂ soil gas flux system (2011 to present; LI-COR Biosciences). Both methods were compared in 2011 and a conversion factor was determined from a linear regression ($y = 0.642x - 32.1$; $r^2 = 0.857$; $P < 0.00001$) to adjust previous measurements via a static chamber (Extended Data Fig. 1b). A respiration collar comprised of a 20-cm-diameter poly(vinyl chloride) ring is permanently installed in each of the 24 plots to a depth of ~4 cm, or within full contact of the mineral soil layer. Freshly fallen litter and herbaceous plants were removed from the respiration collars before each measurement, and collar headspace volume and soil temperature and moisture were recorded (at 5 cm depth). Respiration measurements occurred during the average of the diel phase, or between 10 a.m. and 2 p.m. (Extended Data Fig. 1).

Soil sample collection

Soil samples were collected from each treatment replicate in July 2020. After removing any freshly fallen leaf litter from the soil surface, a 10 cm² of organic horizon ‘brownie’ was quantitatively collected to the depth of the mineral soil (~3.7 cm). Mineral soil was then collected below each organic horizon sample to a depth of 0–10 and 10–20 cm using a Giddings slide hammer corer (5.7 cm diameter) fitted with a specialized sleeve to minimize soil compaction. This resulted in 69 total samples (23 plots × 3 depths). All samples were transported on blue ice to the University of New Hampshire where they were stored at 4 °C until processing within 48 hours of sampling. Intact soil samples were immediately weighed fresh, followed by sieving (<2 mm) and removal of coarse woody debris, roots and rocks larger than 2 mm. Rocks were volumized and subtracted from the total soil core volume. Gravimetric soil moisture was determined by drying subsamples (~5 g) at 65 or 105 °C for organic and mineral soils, respectively. Microbial assays were prioritized for immediate assessment on sieved (<2 mm), homogenized soils, while a subset of soil was air-dried for chemical and physical assays. Sampling access within Harvard Forest is maintained by current filings of Research Project Applications and adherence to making all data collections publicly available within the LTER data archives.

Soil analyses

Soil organic matter concentration and chemistry. Total soil C and N for each of the three depth increments (organic horizon, 0–10 and 10–20 cm mineral soil) was determined on finely ground soils by dry combustion using a PerkinElmer Elemental Analyzer. Paired with bulk density measurements, total C and N stocks (g C m⁻²) were calculated for each treatment replicate (Extended Data Table 2). Solid-state ¹³C-NMR spectroscopy was used to evaluate overall structural changes of SOM in response to the treatments. To minimize the amount of soil collected from our long-term plots where real estate is at a premium, composites were made for each treatment group for both the O horizon and the mineral soil layer (0–10 cm). These composites were from the same set of cores collected to measure the other biogeochemical parameters (soil C and N, root biomass). This approach provides an average representation of how SOM chemistry is altered and is consistent with previous analyses at this experimental site^{18,21,22}. Before NMR analysis, the mineral layer (0–10 cm) samples were repeatedly extracted with hydrogen fluoride (10% v/v) to concentrate the SOM and to also remove iron-bearing soil minerals, which can interfere with the analysis⁴⁹. Samples were analysed by cross polarization–magic angle spinning NMR, using previously published methods⁵⁰. The resulting NMR spectra were integrated into four regions corresponding to

different functional groups: alkyl (0–50 ppm), O-alkyl (50–110 ppm), aromatic and phenolic (110–165 ppm) and carboxyl and carbonyl (165–200 ppm)⁵¹. Each NMR spectrum is an average of thousands of individual replicate scans and solid-state ¹³C-NMR is highly reproducible with measurement errors of ~1% (ref. 52). Integrated areas were normalized to the total NMR signal and expressed as a percentage. Alkyl to O-alkyl carbon ratios were calculated by dividing the integrated area of the alkyl region by the integrated area of the O-alkyl region (Extended Data Table 3)⁵³. The alkyl to O-alkyl carbon ratio increases with progressive SOM decomposition because of the preferential use of O-alkyl carbon by soil microbiota⁵³. Relative differences to the control were calculated as percentages to compare how the experimental treatments altered SOM composition. The relative resistance to decomposition, also referred to as the recalcitrance index⁵⁴, was calculated from the ratio of (alkyl carbon + aromatic and phenolic carbon) to (O-alkyl carbon + carboxylic and carbonyl carbon). This ratio compares the relative quantities of less-preferred substrates such as plant-derived lipids (alkyl carbon) and lignin (aromatic and phenolic carbon) versus preferred substrates such as cellulose (O-alkyl) and carboxylic and carbonyl carbon. With the utilization of cellulose and other more rapidly degraded forms of SOM, this ratio increases, and the overall SOM pool may be more resistant to subsequent decomposition.

Microbial physiology. Microbial growth, turnover and carbon-use efficiency was assessed by ¹⁸O-water incorporation into DNA from an adapted method^{55,56}. Fresh soils were amended with isotopically labelled water, incubated for 24–48 h, sampled for respiration and then total soil DNA was extracted to determine the extent of ¹⁸O-water uptake during microbial growth.

Root analyses. Fine root biomass was estimated by picking live fine roots (<2 mm) from whole soil cores within three days of soil sampling. Soil samples were placed on a 2 mm sieve and roots were carefully removed from the soil. Dead roots were identified and discarded based on their dark discoloration, poor adhesion between the stele and cortex, and brittleness⁵⁷. Fine roots were cleaned with deionized water to remove soil and organic debris, dried at 60 °C and weighed. Dry root tissue N content was determined on finely ground roots by dry combustion using a PerkinElmer 2400 Series II CHN Elemental Analyzer. Total fine root biomass was calculated on a volumetric basis using soil bulk density and expressed as g m⁻². Fine root respiration was measured on roots (<2 mm in size) excised monthly (May to July 2021) from within the organic horizon. Roots were immediately sealed on site within half-pint Mason jars connected to a LI-COR LI-8100-a gas flux system. Respiration was measured over a 5 min duration and root CO₂ fluxes were calculated from the exponential slope phase^{58,59}. Roots were retained for mass determination after drying at 60 °C for 24 h. Ecosystem root respiration was calculated from mass-specific root respiration normalized to total root biomass for a given treatment plot^{58,60}.

Data analysis

Total annual soil CO₂ fluxes were determined by modelling instantaneous respiration rates as a function of soil temperature at the time of sampling, using the resulting model parameters and continuous, hourly measurements of soil temperature to estimate hourly soil CO₂ flux, and then summing estimated hourly fluxes across the entire year (Extended Data Figs. 1a and 3). The model structure was:

$$R_s = Ae^{kT_s}$$

Where R_s represents instantaneous soil respiration in units of mg CO₂·C m⁻² h⁻¹, T_s represents soil temperature (°C) at the time of sampling, and A and k are fitted model parameters. Winter soil respiration was measured for the first few years of the study (2006–2010), where it was determined that winter respiration accounts for 10–14%

of the total annual respiration. It was also determined that performing growing season measurements is adequate for modelling the temperature–respiration response using continuous *in situ* soil temperature data⁴⁶. For every year of the study, we parameterized four of these models to represent each of our four experimental treatments, using instantaneous respiration and temperature measurements from six independent replicate plots in each treatment, except for the warming treatment in which five plots were maintained. To capture a greater range of temperature conditions and respiration rates than would be possible within a single field season, each model included data over a two-year window. That is, each model included data from the year for which we used model parameters to estimate soil respiration as well as data from the preceding year⁸. This approach enabled us to balance the need to capture a range of temperature and respiration rates while also allowing for the temperature dependence of soil respiration to vary with long-term warming⁴¹. Model results are reported in Fig. 1d and Extended Data Table 4. Poor goodness-of-fit ($R^2 < 0.5$) for some treatment × year combinations conforms with earlier studies showing high uncertainty in exponential models of soil respiration as a function of soil temperature that tend to underestimate annual fluxes compared with better fit models⁶². Although more complex models exist to capture the multiple environmental factors that drive soil respiration and facilitate gap-filling and estimation of the total annual flux, these models do not always significantly outperform the simpler exponential model we used⁶². Here, we did not consider environmental factors such as soil moisture because of its relatively small role in explaining variation in soil respiration in this experiment. We assessed the influence of soil temperature and soil moisture on soil respiration by fitting the model $\log(\text{CO}_2 \text{ flux}) = \text{soil temperature} + \text{soil moisture}$ ($P < 0.0001$, $r^2 = 0.47$) and partitioned the relative contribution of each model term using the *lmg* metric in the *relaimpo* package⁶³. This exercise indicated that soil temperature exerted a much stronger influence on soil respiration ($r^2 = 0.42$) compared with soil moisture ($r^2 = 0.05$). The trendlines and confidence intervals in Fig. 1c were generated by fitting the same exponential model structure as above, but across the entire instantaneous respiration dataset rather than using a two-year sliding window to examine thermal acclimation across the whole time series.

Model parameters for each two-year window × treatment combination were used to estimate hourly soil respiration from each plot using continuous, plot-level measurements of hourly soil temperature. In the nitrogen-only treatment, three of the six plots were monitored for hourly temperature measurements, and so $n = 3$ for estimated annual flux and subsequent statistics (the other treatments are monitored for hourly temperature across all plots). Gaps in the temperature record were filled using a two-step procedure, first by taking an average of the remaining plots in a given treatment when individual plot temperatures were not registered or culled during quality assurance and control (QA/QC), and second by linear interpolation across time within individual plots when no plots within a treatment registered temperature measurements (for example, during electrical outages).

For soil biogeochemical analyses, soil subplot duplicate samples were measured separately and then averaged by pooling measured values post biogeochemical analysis. The significance of treatment effects was determined by two-way analysis of variance (ANOVA) comparisons where the best-fit model was assessed, and the significance threshold was set at $P < 0.05$. Normality was tested using the Shapiro–Wilkes test, and data were transformed when necessary. Pairwise differences from control plots were determined by use of Tukey's honestly significant difference (HSD). All statistics were run in R v.3.5.1 (ref. 64).

Differences among treatments in instantaneous soil respiration rates over the course of the experiment were evaluated using a mixed-effects modelling approach⁴⁶ using the *nlme* package⁶⁵ with plot as a random intercept effect and a first-order autocorrelation structure to account for repeated measures. Fixed effects included the treatments warming, nitrogen addition and their combination. Year

was included as a covariate alone and in combination with warming, nitrogen addition and heated × N to examine changes in the experimental treatments over time. Seasonal variation in soil respiration was accounted for in the model with a periodic function that represented sampling dates as radians⁴⁶. Finally, we calculated the log response ratio ($\pm 95\%$ confidence intervals) of treatment to control to further explore the temporal pattern of soil respiration in experimentally manipulated plots relative to controls and to verify our empirical modelling results (Extended Data Fig. 4).

Reporting summary

Further information on research design is available in the Nature Portfolio Reporting Summary linked to this article.

Data availability

Source data, supplemental methods and environmental site data used in this study are publicly available in the files 'soil CO₂ efflux' (hf045-01) and 'soil temperature' (hf045-03) at <https://harvardforest1.fas.harvard.edu/exist/apps/datasets/showData.html?id=HF045>.

Code availability

Code to generate annual respiration modelled in this study is publicly available on the GitHub repository at https://github.com/ewmorr/Knorr_SWaN_model.

References

1. Song, J. et al. A meta-analysis of 1,119 manipulative experiments on terrestrial carbon-cycling responses to global change. *Nat. Ecol. Evol.* **3**, 1309–1320 (2019).
2. Rillig, M. C. et al. The role of multiple global change factors in driving soil functions and microbial biodiversity. *Science* **366**, 886–890 (2019).
3. Georgiou, K. et al. Global stocks and capacity of mineral-associated soil organic carbon. *Nat. Commun.* **13**, 3797 (2022).
4. Pan, Y. et al. A large and persistent carbon sink in the world's forests. *Science* **333**, 988–993 (2011).
5. IPCC. *Climate Change 2023: Synthesis Report. A Contribution of Working Groups I, II and III to the Sixth Assessment Report of the Intergovernmental Panel on Climate Change* (eds Core Writing Team, Lee, H. & Romero, J.) 35–115 (IPCC, 2023).
6. Decina, S. M., Hutyra, L. R. & Templer, P. H. Hotspots of nitrogen deposition in the world's urban areas: a global data synthesis. *Front. Ecol. Environ.* **18**, 92–100 (2019).
7. Zhou, Z., Wang, C. & Luo, Y. Meta-analysis of the impacts of global change factors on soil microbial diversity and functionality. *Nat. Commun.* **11**, 3072 (2020).
8. Melillo, J. M. et al. Long-term pattern and magnitude of soil carbon feedback to the climate system in a warming world. *Science* **358**, 101–105 (2017).
9. Soong, J. L. et al. Five years of whole-soil warming led to loss of subsoil carbon stocks and increased CO₂ efflux. *Sci. Adv.* **7**, eabd1343 (2021).
10. Frey, S. D. et al. Chronic nitrogen additions suppress decomposition and sequester soil carbon in temperate forests. *Biogeochemistry* **121**, 305–316 (2014).
11. Pregitzer, K. S., Burton, A. J., Zak, D. R. & Talhelm, A. F. Simulated chronic nitrogen deposition increases carbon storage in Northern Temperate forests. *Glob. Chang. Biol.* **14**, 142–153 (2008).
12. Liu, L. & Greaver, T. L. A global perspective on belowground carbon dynamics under nitrogen enrichment. *Ecol. Lett.* **13**, 819–828 (2010).
13. Zak, D. R., Pregitzer, K. S., Burton, A. J., Edwards, I. P. & Kellner, H. Microbial responses to a changing environment: implications for the future functioning of terrestrial ecosystems. *Fungal Ecol.* **4**, 386–395 (2011).

14. Lovett, G. M. et al. Nitrogen addition increases carbon storage in soils, but not in trees, in an Eastern U.S. deciduous forest. *Ecosystems* **16**, 980–1001 (2013).
15. Wang, J. J. et al. Long-term nitrogen addition suppresses microbial degradation, enhances soil carbon storage, and alters the molecular composition of soil organic matter. *Biogeochemistry* **142**, 299–313 (2019).
16. Bradford, M. A. et al. Cross-biome patterns in soil microbial respiration predictable from evolutionary theory on thermal adaptation. *Nat. Ecol. Evol.* **3**, 223–231 (2019).
17. Wang, M. et al. Global soil profiles indicate depth-dependent soil carbon losses under a warmer climate. *Nat. Commun.* **13**, 5514 (2022).
18. Pisani, O., Frey, S. D., Simpson, A. J. & Simpson, M. J. Soil warming and nitrogen deposition alter soil organic matter composition at the molecular-level. *Biogeochemistry* **123**, 391–409 (2015).
19. Zak, D. R. et al. Anthropogenic N deposition increases soil organic matter accumulation without altering its biochemical composition. *Glob. Chang. Biol.* **23**, 933–944 (2017).
20. Wang, J. J. et al. Long-term nitrogen addition alters the composition of soil-derived dissolved organic matter. *ACS Earth Space Chem.* **4**, 189–201 (2020).
21. vandenEnden, L., Anthony, M. A., Frey, S. D. & Simpson, M. J. Biogeochemical evolution of soil organic matter composition after a decade of warming and nitrogen addition. *Biogeochemistry* **156**, 161–175 (2021).
22. Stoica, I. et al. Chronic warming and nitrogen-addition alters soil organic matter molecular composition distinctly in tandem compared to individual stressors. *ACS Earth Space Chem.* **7**, 609–622 (2023).
23. Frey, S. D., Knorr, M., Parrent, J. L. & Simpson, R. T. Chronic nitrogen enrichment affects the structure and function of the soil microbial community in temperate hardwood and pine forests. *For. Ecol. Manage.* **196**, 159–171 (2004).
24. Anthony, M. A., Knorr, M., Moore, J. A. M., Simpson, M. & Frey, S. D. Fungal community and functional responses to soil warming are greater than for soil nitrogen enrichment. *Elem. Sci. Anth.* **9**, 000059 (2021).
25. Garcia, M. O. et al. Soil microbes trade-off biogeochemical cycling for stress tolerance traits in response to year-round climate change. *Front. Microbiol.* **11**, 616 (2020).
26. Jansson, J. K. & Hofmockel, K. S. Soil microbiomes and climate change. *Nat. Rev. Microbiol.* **18**, 35–46 (2020).
27. Morrison, E. W. et al. Warming alters fungal communities and litter chemistry with implications for soil carbon stocks. *Soil Biol. Biochem.* **132**, 120–130 (2019).
28. Cheng, L. et al. Warming enhances old organic carbon decomposition through altering functional microbial communities. *ISME J.* **11**, 1825–1835 (2017).
29. Moore, J. A. M. et al. Fungal community structure and function shifts with atmospheric nitrogen deposition. *Glob. Chang. Biol.* **27**, 1349–1364 (2020).
30. Lilleskov, E. A., Kuyper, T. W., Bidartondo, M. I. & Hobbie, E. A. Atmospheric nitrogen deposition impacts on the structure and function of forest mycorrhizal communities: a review. *Environ. Pollut.* **246**, 148–162 (2019).
31. Zhang, T., Chen, H. Y. H. & Ruan, H. Global negative effects of nitrogen deposition on soil microbes. *ISME J.* **12**, 1817–1825 (2018).
32. Morrison, E. W. et al. Chronic nitrogen additions fundamentally restructure the soil fungal community in a temperate forest. *Fungal Ecol.* **23**, 48–57 (2016).
33. Tunison, R., Wood, T., Reed, S. & Cavalieri, M. Respiratory acclimation of tropical forest roots in response to in situ experimental warming and hurricane disturbance. *Ecosystems* **27**, 168–184 (2024).
34. Burton, A., Pregitzer, K., Ruess, R., Hendrick, R. & Allen, M. Root respiration in North American forests: effects of nitrogen concentration and temperature across biomes. *Oecologia* **131**, 559–568 (2002).
35. Burton, A. J., Melillo, J. M. & Frey, S. D. Adjustment of forest ecosystem root respiration as temperature warms. *J. Integr. Plant Biol.* **50**, 1467–1483 (2008).
36. Han, M. & Zhu, B. Linking root respiration to chemistry and morphology across species. *Glob. Chang. Biol.* **27**, 190–201 (2021).
37. Pregitzer, K. S., Laskowski, M. J., Burton, A. J., Lessard, V. C. & Zak, D. R. Variation in sugar maple root respiration with root diameter and soil depth. *Tree Physiol.* **18**, 665–670 (1998).
38. McCormack, L., Adams, T. S., Smithwick, E. A. H. & Eissenstat, D. M. Predicting fine root lifespan from plant functional traits in temperate trees. *New Phytol.* **195**, 823–831 (2012).
39. Bai, T., Wang, P., Qiu, Y., Zhang, Y. & Hu, S. Nitrogen availability mediates soil carbon cycling response to climate warming: a meta-analysis. *Glob. Chang. Biol.* **29**, 2608–2626 (2023).
40. Canarini, A., Kaiser, C., Merchant, A., Richter, A. & Wanek, W. Root exudation of primary metabolites: mechanisms and their roles in plant responses to environmental stimuli. *Front. Plant Sci.* **10**, 157 (2019).
41. Sun, L., Ataka, M., Kominami, Y. & Yoshimura, K. Relationship between fine-root exudation and respiration of two *Quercus* species in a Japanese temperate forest. *Tree Physiol.* **37**, 1011–1020 (2017).
42. Clemmensen, K. E. et al. Carbon sequestration is related to mycorrhizal fungal community shifts during long-term succession in boreal forests. *New Phytol.* **205**, 1525–1536 (2015).
43. Gale, W. J. & Cambardella, C. A. Carbon dynamics of surface residue- and root-derived organic matter under simulated no-till. *Soil Sci. Soc. Am. J.* **64**, 190–195 (2000).
44. Godbold, D. L. et al. Mycorrhizal hyphal turnover as a dominant process for carbon input into soil organic matter. *Plant Soil* **281**, 15–24 (2006).
45. Frey, S. D. Mycorrhizal fungi as mediators of soil organic matter dynamics. *Annu. Rev. Ecol. Evol. Syst.* **50**, 237–259 (2019).
46. Contosta, A. R., Frey, S. D. & Cooper, A. B. Seasonal dynamics of soil respiration and N mineralization in chronically warmed and fertilized soils. *Ecosphere* **2**, 1–21 (2011).
47. Boose, E. *Fisher Meteorological Station at Harvard Forest since 2001*. Harvard Forest Data Archive: HF001v.26 (2021); <https://harvardforest1.fas.harvard.edu/exist/apps/datasets/showData.html?id=HF001>
48. Contosta, A. R., Frey, S. D., Ollinger, S. V. & Cooper, A. B. Soil respiration does not acclimate to warmer temperatures when modeled over seasonal timescales. *Biogeochemistry* **112**, 555–570 (2013).
49. Rumpel, C. et al. Alteration of soil organic matter following treatment with hydrofluoric acid (HF). *Org. Geochem.* **37**, 1437–1451 (2006).
50. Conte, P., Spaccini, R. & Piccolo, A. State of the art of CPMAS ^{13}C -NMR spectroscopy applied to natural organic matter. *Prog. Nucl. Magn. Reson. Spectrosc.* **44**, 215–223 (2004).
51. Preston, C. M. Environmental NMR: solid-state methods. *eMagRes* **3**, 29–42 (2014).
52. Sun, S. et al. Soil warming and nitrogen deposition alter soil respiration, microbial community structure and organic carbon composition in a coniferous forest on eastern Tibetan Plateau. *Geoderma* **353**, 283–292 (2019).
53. Baldock, J. A., Oades, J. M. & Waters, A. G. Aspects of the chemical structure of soil organic materials as revealed by solid-state ^{13}C NMR spectroscopy. *Biogeochemistry* **16**, 1–42 (1992).

54. Ostertag, R., Marín-Spiotta, E., Silver, W. L. & Schulter, J. Litterfall and decomposition in relation to soil carbon pools along a secondary forest chronosequence in Puerto Rico. *Ecosystems* **11**, 701–714 (2008).
55. Spohn, M., Klaus, K., Wanek, W. & Richter, A. Microbial carbon use efficiency and biomass turnover times depending on soil depth – implications for carbon cycling. *Soil Biol. Biochem.* **96**, 74–81 (2016).
56. Spohn, M. et al. Soil microbial carbon use efficiency and biomass turnover in a long-term fertilization experiment in a temperate grassland. *Soil Biol. Biochem.* **97**, 168–175 (2016).
57. Persson, H. A. & Stadenberg, I. Spatial distribution of fine-roots in boreal forests in eastern Sweden. *Plant Soil* **318**, 1–14 (2009).
58. Jarvi, M. P. & Burton, A. J. Root respiration and biomass responses to experimental soil warming vary with root diameter and soil depth. *Plant Soil* **451**, 435–446 (2020).
59. Paradiso, E., Jevon, F. & Matthes, J. Fine root respiration is more strongly correlated with root traits than tree species identity. *Ecosphere* **10**, e02944 (2019).
60. Melillo, J. M. et al. Soil warming, carbon–nitrogen interactions, and forest carbon budgets. *Proc. Natl Acad. Sci. USA* **108**, 9508–9512 (2011).
61. Bradford, M. A. et al. Thermal adaptation of soil microbial respiration to elevated temperature. *Ecol. Lett.* **11**, 1316–1327 (2008).
62. Richardson, A. D. et al. Comparing simple respiration models for eddy flux and dynamic chamber data. *Agric. For. Meteorol.* **141**, 219–234 (2006).
63. Groemping, U. Relative importance for linear regression in R: the package relaimpo. *J. Stat. Softw.* **17**, 1–27 (2006).
64. R v.3.5.1 (R Foundation for Statistical Computing, 2021).
65. R v.3.1.153 (R Foundation for Statistical Computing, 2021).

Acknowledgements

We thank C. Bunyon, E. Johnson, A. Kittle, O. LaChapelle, J. Trombley and C. Williston for assistance with sample collection and analysis. R. Tunison provided insight into methods for measuring fine root respiration. We also thank M. T. Anaraki for completing the phospholipid fatty acid analysis and R. Soong for assistance with acquiring solid-state ¹³C-NMR analysis. The Soil Warming × Nitrogen Addition Study at Harvard Forest is maintained with support from the US National Science Foundation Long Term Ecological Research Program (grant no. DEB-1832110) and a Long-Term Research in Environmental Biology grant (no. DEB-1456610) to S.D.F. M.J.S. acknowledges the Natural Sciences and Engineering Research Council of Canada for support via the Tier 1 Canada Research Chair in Integrative Molecular Biogeochemistry.

Author contributions

S.D.F. conceived the project. A.R.C. and S.D.F. designed and initiated the Soil Warming × Nitrogen Addition Study at Harvard Forest in 2006. M.A.K. maintained the experiment, collected the monthly soil respiration data and collaborated with A.R.C. and E.W.M. to estimate annual soil CO₂ fluxes. T.J.M., M.A.K. and S.D.F. collected the soil samples. T.J.M. processed the samples for root biomass and M.A.K. assisted T.J.M. with soil nutrient analyses. K.M.G. and M.A.A. conducted microbial analyses and assisted with data interpretation. I.S. and M.J.S. conducted the NMR analyses and assisted with their interpretation. M.A.K. wrote the initial manuscript draft, with input from S.D.F. All authors reviewed and contributed to the manuscript.

Competing interests

The authors declare no competing interests.

Additional information

Extended data is available for this paper at
<https://doi.org/10.1038/s41559-024-02546-x>.

Supplementary information The online version contains supplementary material available at
<https://doi.org/10.1038/s41559-024-02546-x>.

Correspondence and requests for materials should be addressed to Melissa A. Knorr or S. D. Frey.

Peer review information *Nature Ecology & Evolution* thanks Shuijin Hu, Zhongkui Luo and the other, anonymous, reviewer(s) for their contribution to the peer review of this work. Peer reviewer reports are available.

Reprints and permissions information is available at www.nature.com/reprints.

Publisher's note Springer Nature remains neutral with regard to jurisdictional claims in published maps and institutional affiliations.

Springer Nature or its licensor (e.g. a society or other partner) holds exclusive rights to this article under a publishing agreement with the author(s) or other rightsholder(s); author self-archiving of the accepted manuscript version of this article is solely governed by the terms of such publishing agreement and applicable law.

© The Author(s), under exclusive licence to Springer Nature Limited 2024

¹Center for Soil Biogeochemistry and Microbial Ecology, University of New Hampshire, Durham, NH, USA. ²Department of Natural Resources and the Environment, University of New Hampshire, Durham, NH, USA. ³Earth Systems Research Center, Institute for the Study of Earth, Oceans, and Space, University of New Hampshire, Durham, NH, USA. ⁴Center for Microbiology and Environmental Systems Science, University of Vienna, Vienna, Austria.

⁵Department of Physical and Environmental Sciences and Environmental NMR Centre, University of Toronto Scarborough, Toronto, Ontario, Canada.

⁶Department of Environmental Science and Sustainability, Allegheny College, Meadville, PA, USA. ✉e-mail: mel.knorr@unh.edu; serita.frey@unh.edu

Extended Data Table 1 | Type III sum of squares model output for the linear mixed effects model used to test for differences in instantaneous respiration due to experimental treatments across time

Model Term	F-value	p-value
Intercept	19.70	< 0.0001
Heated	6.13	0.022
Nitrogen	3.01	0.098
Year	26.62	< 0.0001
$\sin(2 \times \pi \times \text{DOY})^a$	1444.69	< 0.0001
$\cos(2 \times \pi \times \text{DOY})^a$	2087.09	< 0.0001
Heated \times Nitrogen	7.51	0.013
Heated \times Year	6.07	0.014
Nitrogen \times Year	2.99	0.084
Heated \times Nitrogen \times Year	7.52	0.006

^aThe model terms $\sin(2 \times \pi \times \text{DOY})$ and $\cos(2 \times \pi \times \text{DOY})$ together represent the periodic function used to represent the seasonal variation in soil respiration⁴⁶. Here DOY is the ordinal day of year calculated as a radian.

Extended Data Table 2 | Soil carbon and nitrogen stocks, organic horizon mass, and soil bulk density

Experimental treatment				
Response variable	Control	Nitrogen	Heated	Heated x N
Soil C stock: g C m ⁻²				
Forest floor	3646 (295) ^{ab}	3785 (452) ^a	1970 (140) ^c	2472 (246) ^{bcd}
0-10 cm mineral soil	2641 (196)	2678 (191)	2410 (146)	2851 (180)
10-20 cm mineral soil	1734 (146)	2527 (216)*	1807 (217)	2357 (416)*
Total soil profile	8021 (165) ^a	8990 (441) ^a	6187 (387) ^b	7680 (671) ^{ab}
Soil N stock: g N m ⁻²				
Forest floor	151 (13) ^a	151 (17) ^a	84 (6) ^b	102 (8) ^b
0-10 cm mineral soil	129 (15)	132 (9)	116 (8)	139 (8)
10-20 cm mineral soil	82 (9)	125 (10)*	93 (17)	114 (18)*
Total soil profile	361 (15)	408 (19)	294 (26)	355 (27)
Organic mass: kg m ⁻²				
Forest floor	13 (2)	14 (2)	10 (1)	10 (1)
Bulk density: g cm ⁻³				
0-10 cm	0.50 (0.02)	0.51 (0.04)	0.46 (0.04)	0.52 (0.03)
10-20 cm	0.53 (0.01)	0.67 (0.06)	0.57 (0.04)	0.57 (0.05)

Soil C and N concentrations were determined via dry combustion on an elemental analyzer and then adjusted to a volumetric basis (that is, stock) using bulk density. Lowercase letters denote significant pairwise comparisons between treatments ($P < 0.05$), derived from two-way ANOVA and Tukey HSD. Asterisks for the SOC and SON 10–20 cm depth increment stocks indicate a main effect of nitrogen, $P = 0.023$, $P = 0.030$ respectively.

Extended Data Table 3 | Solid-state ^{13}C nuclear magnetic resonance (NMR) spectroscopy integration values for the main regions corresponding to soil organic matter compositional categories

	Alkyl C	O-alkyl C	Aromatic + phenolic C	Carboxylic + carbonyl C	Relative decomposition stage ^a	Relative resistance to decomposition ^b
Forest Floor						
Control	30	49	16	5	0.61	0.85
Nitrogen	28	51	16	6	0.55	0.77
Heat	32	49	14	5	0.65	0.85
Heated x N	34	47	15	4	0.72	0.96
Mineral soil (0-10 cm)						
Control	40	36	17	7	1.11	1.33
Nitrogen	36	39	18	7	0.92	1.17
Heat	40	36	18	6	1.11	1.38
Heated x N	41	36	17	6	1.14	1.38

^aRelative stage of decomposition is calculated as the alkyl carbon/O-alkyl carbon ratio which increases with progressive soil organic matter decomposition⁵³. ^bRelative resistance to decomposition is calculated as (alkyl carbon + aromatic & phenolic carbon) / (O-alkyl carbon+ carboxylic & carbonyl carbon); this ratio compares different soil organic matter components and their potential substrates, with higher ratios suggesting a shift in the overall soil organic matter composition to less preferred substrates which may be more resistant to decomposition⁵⁴.

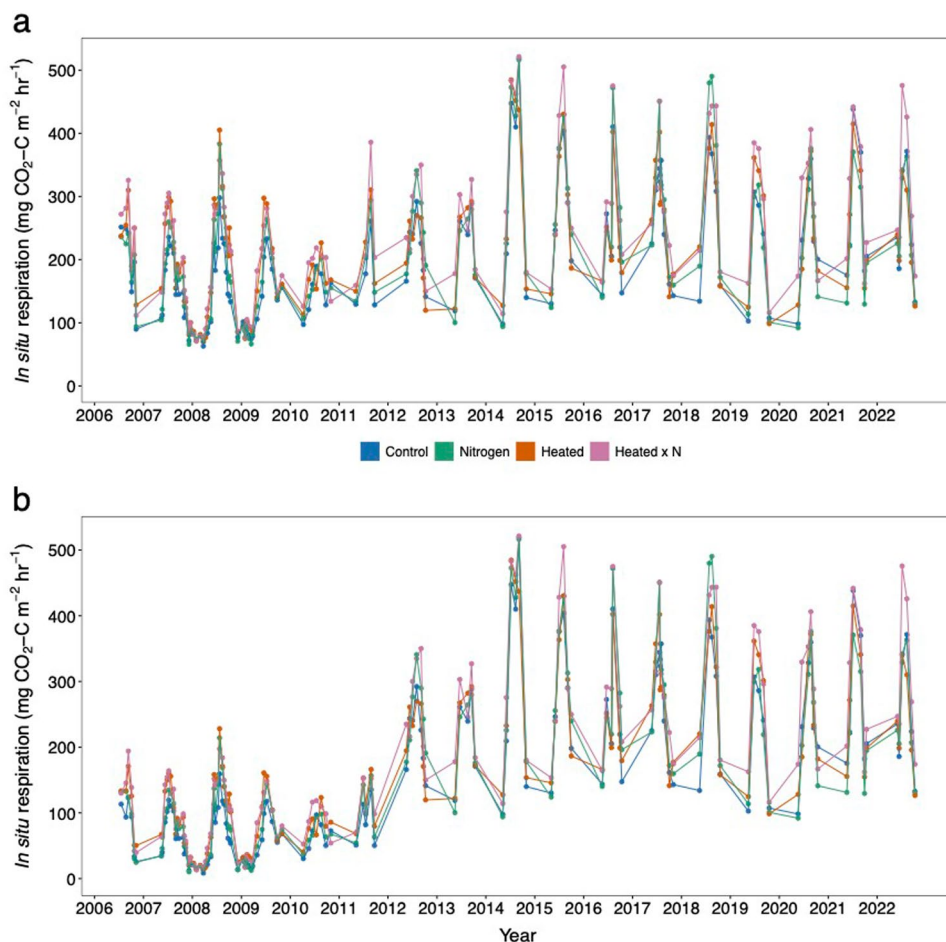
Extended Data Table 4 | Results from temperature-respiration linear regression models for each year x treatment combination

Year	Treatment	A	A.SE	A.t	A.p	k	k.SE	k.t	k.p	χ^2	df
2007	C	4.230	0.052	80.857	<0.00001	0.058	0.004	16.027	<0.00001	0.674	124
2007	N	4.244	0.046	92.160	<0.00001	0.060	0.003	19.426	<0.00001	0.756	122
2007	H	4.233	0.072	58.660	<0.00001	0.055	0.004	14.116	<0.00001	0.616	124
2007	HN	4.129	0.066	62.212	<0.00001	0.060	0.003	17.159	<0.00001	0.704	124
2008	C	4.203	0.031	135.495	<0.00001	0.060	0.002	25.778	<0.00001	0.773	195
2008	N	4.220	0.032	133.222	<0.00001	0.068	0.002	28.875	<0.00001	0.812	193
2008	H	4.005	0.049	82.185	<0.00001	0.069	0.003	24.750	<0.00001	0.758	196
2008	HN	4.022	0.044	90.558	<0.00001	0.066	0.002	27.201	<0.00001	0.793	193
2009	C	4.242	0.037	114.895	<0.00001	0.058	0.003	19.924	<0.00001	0.706	165
2009	N	4.312	0.036	118.267	<0.00001	0.064	0.003	22.519	<0.00001	0.757	163
2009	H	4.024	0.051	78.462	<0.00001	0.069	0.003	22.141	<0.00001	0.744	169
2009	HN	4.009	0.050	80.876	<0.00001	0.067	0.003	23.628	<0.00001	0.771	166
2010	C	4.434	0.072	61.945	<0.00001	0.037	0.005	7.254	<0.00001	0.347	99
2010	N	4.550	0.059	76.843	<0.00001	0.036	0.004	8.665	<0.00001	0.434	98
2010	H	4.355	0.085	51.062	<0.00001	0.041	0.005	8.542	<0.00001	0.432	96
2010	HN	4.200	0.079	53.467	<0.00001	0.050	0.004	11.993	<0.00001	0.583	103
2011	C	4.365	0.149	29.204	<0.00001	0.044	0.009	4.698	0.00001	0.245	68
2011	N	4.373	0.135	32.283	<0.00001	0.048	0.008	5.822	<0.00001	0.329	69
2011	H	4.566	0.223	20.496	<0.00001	0.033	0.011	3.019	0.00377	0.136	58
2011	HN	4.175	0.143	29.289	<0.00001	0.052	0.007	7.875	<0.00001	0.470	70
2012	C	4.372	0.162	26.912	<0.00001	0.054	0.010	5.568	<0.00001	0.313	68
2012	N	4.540	0.205	22.133	<0.00001	0.051	0.012	4.203	0.00008	0.204	69
2012	H	4.259	0.154	27.574	<0.00001	0.055	0.008	7.214	<0.00001	0.473	58
2012	HN	4.508	0.155	29.023	<0.00001	0.046	0.008	6.075	<0.00001	0.345	70
2013	C	4.367	0.150	29.096	<0.00001	0.062	0.010	6.456	<0.00001	0.377	69
2013	N	4.311	0.202	21.325	<0.00001	0.070	0.013	5.389	<0.00001	0.296	69
2013	H	4.135	0.154	26.855	<0.00001	0.063	0.008	7.986	<0.00001	0.524	58
2013	HN	4.446	0.164	27.069	<0.00001	0.053	0.008	6.295	<0.00001	0.361	70
2014	C	3.591	0.154	23.375	<0.00001	0.130	0.011	12.331	<0.00001	0.704	64
2014	N	3.609	0.189	19.072	<0.00001	0.128	0.013	9.970	<0.00001	0.612	63
2014	H	3.127	0.220	14.206	<0.00001	0.124	0.011	10.924	<0.00001	0.692	53
2014	HN	3.592	0.214	16.776	<0.00001	0.104	0.011	9.469	<0.00001	0.587	63
2015	C	3.734	0.150	24.914	<0.00001	0.126	0.010	12.362	<0.00001	0.689	69
2015	N	3.913	0.177	22.082	<0.00001	0.115	0.012	9.689	<0.00001	0.584	67
2015	H	3.260	0.204	15.987	<0.00001	0.124	0.011	11.495	<0.00001	0.695	58
2015	HN	3.675	0.226	16.261	<0.00001	0.103	0.011	8.967	<0.00001	0.542	68
2016	C	4.368	0.167	26.181	<0.00001	0.072	0.011	6.682	<0.00001	0.393	69
2016	N	4.426	0.189	23.384	<0.00001	0.073	0.012	5.906	<0.00001	0.339	68
2016	H	4.121	0.243	16.962	<0.00001	0.071	0.013	5.588	<0.00001	0.350	58
2016	HN	4.170	0.244	17.119	<0.00001	0.072	0.012	5.922	<0.00001	0.340	68
2017	C	4.274	0.141	30.279	<0.00001	0.070	0.009	8.045	<0.00001	0.444	81
2017	N	4.349	0.163	26.685	<0.00001	0.069	0.010	6.973	<0.00001	0.372	82
2017	H	4.187	0.227	18.472	<0.00001	0.063	0.011	5.569	<0.00001	0.310	69
2017	HN	4.345	0.193	22.511	<0.00001	0.059	0.009	6.225	<0.00001	0.324	81
2018	C	4.219	0.153	27.646	<0.00001	0.073	0.009	8.140	<0.00001	0.469	75
2018	N	4.169	0.144	28.914	<0.00001	0.084	0.008	9.926	<0.00001	0.565	76
2018	H	4.037	0.223	18.112	<0.00001	0.073	0.011	6.755	<0.00001	0.416	64

Extended Data Table 4 (continued) | Results from temperature-respiration linear regression models for each year x treatment combination

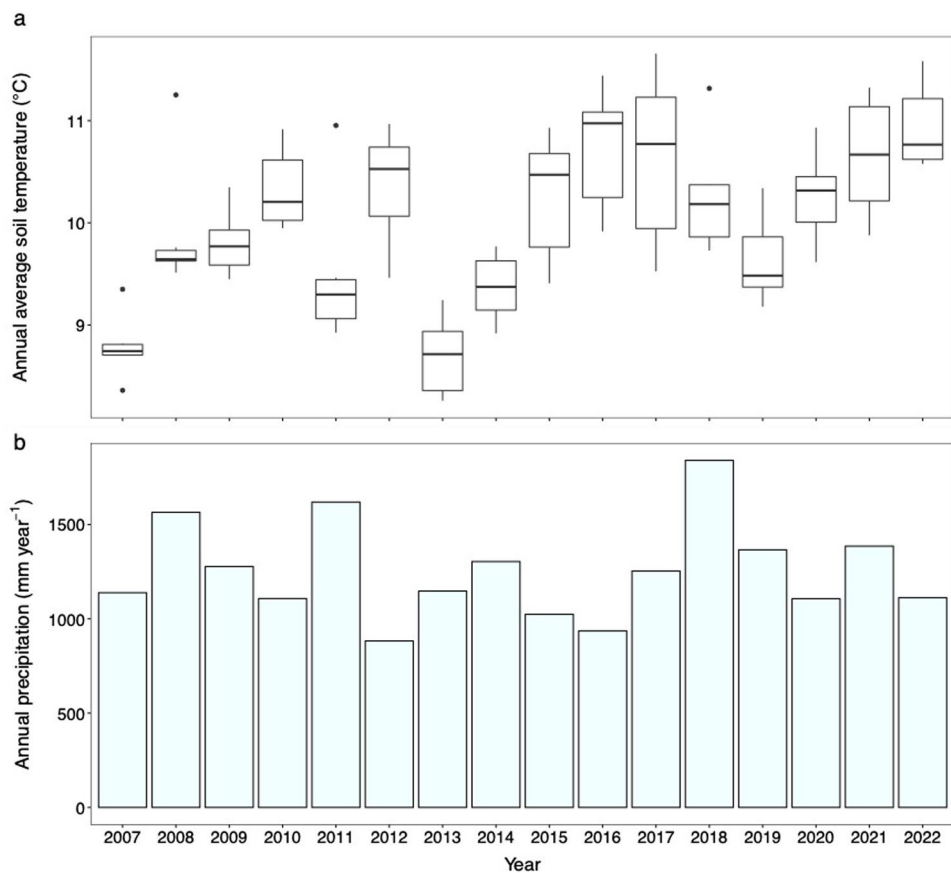
2018	HN	4.198	0.186	22.565	<0.00001	0.068	0.009	7.675	<0.00001	0.437	76
2019	C	3.918	0.145	26.945	<0.00001	0.085	0.008	10.235	<0.00001	0.644	58
2019	N	3.933	0.131	29.968	<0.00001	0.093	0.008	12.269	<0.00001	0.722	58
2019	H	3.425	0.189	18.158	<0.00001	0.105	0.009	11.106	<0.00001	0.720	48
2019	HN	3.827	0.139	27.534	<0.00001	0.090	0.007	13.132	<0.00001	0.748	58
2020	C	3.654	0.184	19.850	<0.00001	0.098	0.011	9.097	<0.00001	0.564	64
2020	N	3.545	0.168	21.089	<0.00001	0.104	0.010	10.598	<0.00001	0.637	64
2020	H	3.338	0.225	14.857	<0.00001	0.100	0.011	9.167	<0.00001	0.613	53
2020	HN	3.925	0.199	19.754	<0.00001	0.079	0.010	8.156	<0.00001	0.510	64
2021	C	3.196	0.334	9.560	<0.00001	0.132	0.020	6.650	<0.00001	0.391	69
2021	N	2.719	0.288	9.428	<0.00001	0.156	0.017	9.107	<0.00001	0.546	69
2021	H	3.409	0.289	11.790	<0.00001	0.096	0.014	7.025	<0.00001	0.460	58
2021	HN	3.619	0.335	10.791	<0.00001	0.092	0.016	5.837	<0.00001	0.327	70
2022	C	3.326	0.266	12.504	<0.00001	0.130	0.016	8.006	<0.00001	0.482	69
2022	N	3.268	0.244	13.371	<0.00001	0.129	0.015	8.704	<0.00001	0.523	69
2022	H	3.761	0.313	12.030	<0.00001	0.081	0.015	5.362	<0.00001	0.331	58
2022	HN	3.361	0.329	10.201	<0.00001	0.108	0.016	6.814	<0.00001	0.399	70

Abbreviations: A (intercept), k (slope), SE (standard error), t (t value), p (p value), df (degrees of freedom). Treatment designations (C = Control, N = Nitrogen, H = Heated, HN = Heated x N).


Extended Data Fig. 1 | Field measured, instantaneous CO₂ flux.

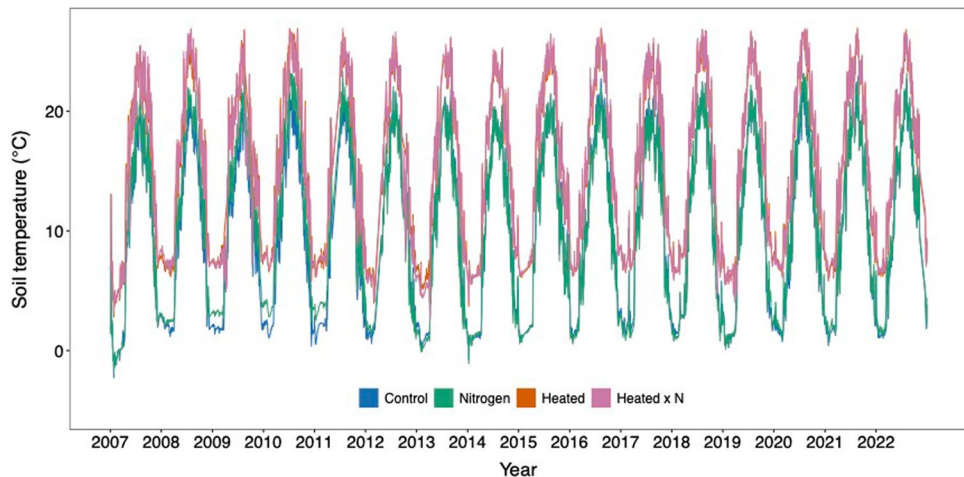
a, Measurements in 2006 – 2011 were made via static chamber and these data were corrected for direct comparison with the LI-COR method used post-2011 (see Methods). Annual fluxes were modeled from these data. **b**, measurements in 2006 – 2011 have not been adjusted with the conversion factor. Post 2011, all

data are measured via LI-COR and not corrected for either panel. Points are dates of measurement. A linear mixed effects model was used to test for differences in instantaneous respiration due to experimental treatments across time (see Extended Data Table 1).

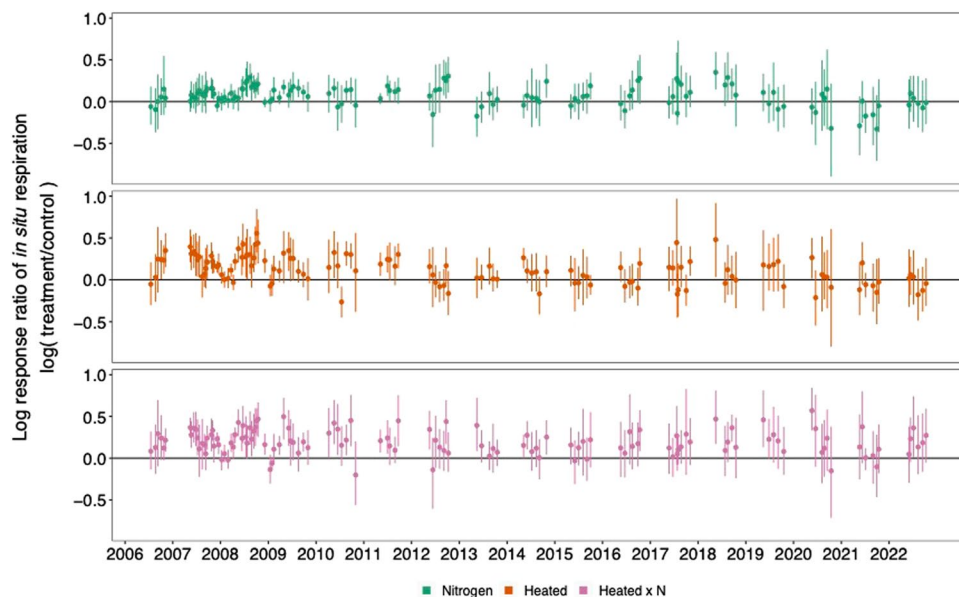


Extended Data Fig. 2 | Ambient climate conditions. a, Annual average soil temperature at 5 cm depth in the control treatment ($n = 6$), monitored and recorded every 10 minutes via datalogger. The boxplot centre line indicates the median, the box indicates the 25th and 75th percentiles (IQR, interquartile range),

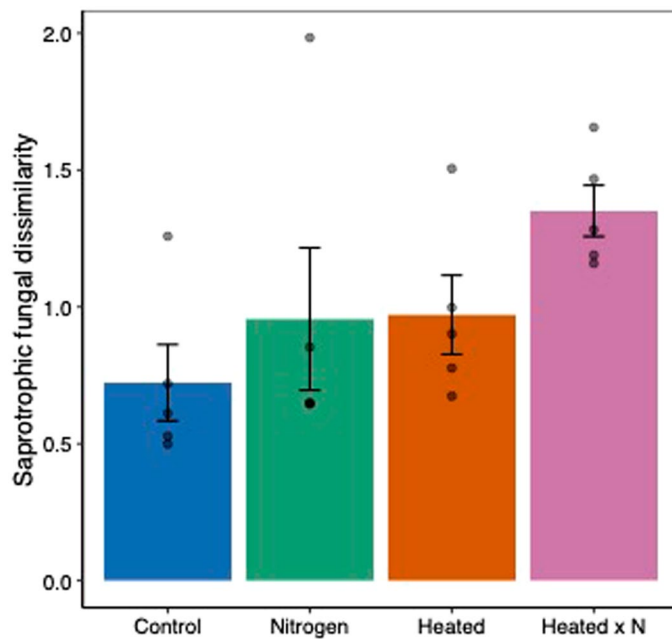
and the whiskers indicate the smallest and largest value within 1.5×IQR. Outliers beyond 1.5×IQR are indicated by points. b, annual precipitation (rain + snow) as monitored by the Harvard Forest Meteorological Station (<https://doi.org/10.6073/pasta/a0083f14a6475b78b0bbb2abf26eb295>).



Extended Data Fig. 3 | Soil temperature at 5 cm mineral soil depth. Temperatures are automatically and continuously recorded every 10 minutes to monitor the heating cable system and to maintain a 5 °C difference between warmed and unwarmed plots.

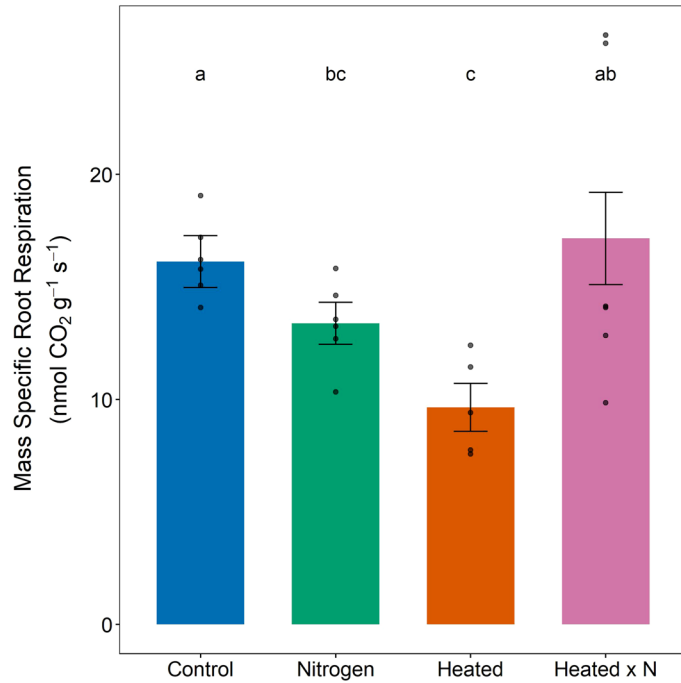


Extended Data Fig. 4 | Log response ratio of *in situ* respiration. Means and 95% confidence intervals were estimated from 9,999 bootstrap resamples of the instantaneous respiration data.



Extended Data Fig. 5 | Saprotrophic fungal community composition across treatments. Fungal community dissimilarity represented as the first non-metric multidimensional scaling ordination axis (mean \pm SE; n = 5 for all treatments) capturing variation in Bray-Curtis dissimilarity computed from relative

abundance of 97% ITS2 operational taxonomic units (OTUs). Permutation-based analysis of variance (PERMANOVA) shows a significant effect of heating ($F(3,16) = 1.85, P = 0.009$) and heating \times N ($F(3,16) = 1.61, P = 0.02$).



Extended Data Fig. 6 | Mass-specific root CO₂ flux. Root respiration per gram weight of roots (mean \pm SE) from all treatments for months May – July, 2021 ($n = 6$ for all treatments except the heated treatment where $n = 5$). Two-way ANOVA and Tukey HSD (control:nitrogen $P = 0.046$, control:heated $P = 0.0008$, heated:heated x N $P = 0.0057$).

Reporting Summary

Nature Portfolio wishes to improve the reproducibility of the work that we publish. This form provides structure for consistency and transparency in reporting. For further information on Nature Portfolio policies, see our [Editorial Policies](#) and the [Editorial Policy Checklist](#).

Statistics

For all statistical analyses, confirm that the following items are present in the figure legend, table legend, main text, or Methods section.

n/a Confirmed

- The exact sample size (n) for each experimental group/condition, given as a discrete number and unit of measurement
- A statement on whether measurements were taken from distinct samples or whether the same sample was measured repeatedly
- The statistical test(s) used AND whether they are one- or two-sided
Only common tests should be described solely by name; describe more complex techniques in the Methods section.
- A description of all covariates tested
- A description of any assumptions or corrections, such as tests of normality and adjustment for multiple comparisons
- A full description of the statistical parameters including central tendency (e.g. means) or other basic estimates (e.g. regression coefficient) AND variation (e.g. standard deviation) or associated estimates of uncertainty (e.g. confidence intervals)
- For null hypothesis testing, the test statistic (e.g. F , t , r) with confidence intervals, effect sizes, degrees of freedom and P value noted
Give P values as exact values whenever suitable.
- For Bayesian analysis, information on the choice of priors and Markov chain Monte Carlo settings
- For hierarchical and complex designs, identification of the appropriate level for tests and full reporting of outcomes
- Estimates of effect sizes (e.g. Cohen's d , Pearson's r), indicating how they were calculated

Our web collection on [statistics for biologists](#) contains articles on many of the points above.

Software and code

Policy information about [availability of computer code](#)

Data collection	Real-time measurements of soil temperature and soil moisture are collected via Campbell Scientific Loggernet software
Data analysis	Code to generate annual respiration modeled in this study is publicly available on GitHub repository at the following URL address: https://github.com/ewmorr/Knorr_SWaN_model

For manuscripts utilizing custom algorithms or software that are central to the research but not yet described in published literature, software must be made available to editors and reviewers. We strongly encourage code deposition in a community repository (e.g. GitHub). See the Nature Portfolio [guidelines for submitting code & software](#) for further information.

Data

Policy information about [availability of data](#)

All manuscripts must include a [data availability statement](#). This statement should provide the following information, where applicable:

- Accession codes, unique identifiers, or web links for publicly available datasets
- A description of any restrictions on data availability
- For clinical datasets or third party data, please ensure that the statement adheres to our [policy](#)

Source data, supplemental methods, and environmental site data used in this study are publicly available at the following files at the URL address below; soil CO₂ efflux (hf045-01) and soil temperature (hf045-03):

Research involving human participants, their data, or biological material

Policy information about studies with [human participants or human data](#). See also policy information about [sex, gender \(identity/presentation\), and sexual orientation](#) and [race, ethnicity and racism](#).

Reporting on sex and gender	n/a
Reporting on race, ethnicity, or other socially relevant groupings	n/a
Population characteristics	n/a
Recruitment	n/a
Ethics oversight	n/a

Note that full information on the approval of the study protocol must also be provided in the manuscript.

Field-specific reporting

Please select the one below that is the best fit for your research. If you are not sure, read the appropriate sections before making your selection.

Life sciences Behavioural & social sciences Ecological, evolutionary & environmental sciences

For a reference copy of the document with all sections, see nature.com/documents/nr-reporting-summary-flat.pdf

Ecological, evolutionary & environmental sciences study design

All studies must disclose on these points even when the disclosure is negative.

Study description	The experimental design consists of 24, 3 m ² plots with six replicates each of four treatments: Control which receives no manipulation; Heated where soil is warmed continuously to 5°C above ambient soil temperatures by buried resistance cables; Nitrogen where treatment plots receive an aqueous addition of NH ₄ NO ₃ at a rate of 50 kg N ha ⁻¹ yr ⁻¹ applied in six monthly doses throughout the growing season (May – Oct); and Heated x N which receives both warming (+5°C) and N addition (50 kg N ha ⁻¹ yr ⁻¹)
Research sample	Soil samples were collected after removing any freshly fallen leaf litter from the soil surface, a 10 cm ² organic horizon sample was quantitatively collected to the depth of the mineral soil (~3.7 cm). Mineral soil was then collected below each organic horizon sample to a depth of 0-10 and 10-20 cm using a Giddings™ slide hammer corer (5.7 cm diameter) fitted with a specialized sleeve to minimize soil compaction
Sampling strategy	Soils are sampled in replicate order, 1 - 6, to ensure randomization of treatment plots. Soil sample size is restricted to 10 cm square organic horizon and ~6 cm width cores to minimize oversampling of the 3 x 3 m plot sizes
Data collection	Sampling was accomplished by M.A. Knorr, S.D. Frey, and T.J. Muratore. Data collection of post processed soils was accomplished by M.A. Knorr, T.J. Muratore, M.A. Anthony, K.M. Geyer, I. Stoica, and M. Simpson. Data modeling and code generation was accomplished by A.R. Contosta and E.W. Morrison
Timing and spatial scale	All organic and mineral soils were sampled within one day in July of 2020 with a 3 person team to expedite sampling. Samples were then transported on blue ice to the University of New Hampshire where all time sensitive assays were completed within 48 hours of sample collection
Data exclusions	No data were excluded
Reproducibility	Standard ecological field replication was adhered to
Randomization	Field design for this experiment is fully randomized
Blinding	All samples were given a unique, non-descriptive identifier so as not to confer treatment conditions

Did the study involve field work? Yes No

Field work, collection and transport

Field conditions	This is an even aged, mixed deciduous forest dominated by American beech (<i>Fagus grandifolia</i>), white birch (<i>Betula papyrifera</i>), red maple (<i>Acer rubrum</i> L.), striped maple (<i>A. pensylvanicum</i> L.), red oak (<i>Quercus rubra</i>), and black oak (<i>Q. velutina</i> Lam.). Mean annual temperature is 7°C but can vary from a high of 32°C in summer to a low of -25°C in winter. Mean annual precipitation is evenly distributed across the year, averaging 1100 mm. Soils are fine loamy, mixed, mesic Typic Dystrudepts of the Gloucester series with pH of 3.8 and 4.3 in the organic horizon and mineral soil (0-10 cm), respectively.
Location	The Soil Warming × Nitrogen Addition Study, initiated in 2006, is located at the Harvard Forest Long-term Ecological Research (LTER) site in Petersham, MA, USA (42°50'.5315°N, 72°18'.1900°W)
Access & import/export	Access to the Harvard Forest Long-term Ecological research site is maintained by current filings of Research Project Applications and adherence to making all data collections publicly available within the Harvard Forest data archives
Disturbance	No disturbance was caused

Reporting for specific materials, systems and methods

We require information from authors about some types of materials, experimental systems and methods used in many studies. Here, indicate whether each material, system or method listed is relevant to your study. If you are not sure if a list item applies to your research, read the appropriate section before selecting a response.

Materials & experimental systems

n/a	Involved in the study
<input checked="" type="checkbox"/>	<input type="checkbox"/> Antibodies
<input checked="" type="checkbox"/>	<input type="checkbox"/> Eukaryotic cell lines
<input checked="" type="checkbox"/>	<input type="checkbox"/> Palaeontology and archaeology
<input checked="" type="checkbox"/>	<input type="checkbox"/> Animals and other organisms
<input checked="" type="checkbox"/>	<input type="checkbox"/> Clinical data
<input checked="" type="checkbox"/>	<input type="checkbox"/> Dual use research of concern
<input type="checkbox"/>	<input checked="" type="checkbox"/> Plants

Methods

n/a	Involved in the study
<input checked="" type="checkbox"/>	<input type="checkbox"/> ChIP-seq
<input checked="" type="checkbox"/>	<input type="checkbox"/> Flow cytometry
<input checked="" type="checkbox"/>	<input type="checkbox"/> MRI-based neuroimaging